Journal of The Electrochemical Society, **153** (5) A897-A901 (2006)
0013-4651/2006/153(5)/A897/5/$20.00 © The Electrochemical Society

Performance of an Intermediate-Temperature Fuel Cell Using a Proton-Conducting $Sn_{0.9}In_{0.1}P_2O_7$ Electrolyte

Pilwon Heo, Hidetaka Shibata, Masahiro Nagao,* Takashi Hibino,,z and Mitsuru Sano**

Graduate School of Environmental Studies, Nagoya University, Nagoya 464-8601, Japan

Performance of a fuel cell using $Sn_{0.9}In_{0.1}P_2O_7$ as the electrolyte was evaluated in the temperature range of 150–300°C under unhumidified conditions. The IR drop and electrode overpotential of the cell were measured separately by the current interruption method. The dc conductivity values of the electrolyte between 150 and 300°C, estimated from the IR drop, were comparable to the ac conductivity values (1.48×10^{-1}–1.95×10^{-1} S cm^{-1}) of the electrolyte. The cell performance was improved by forming an intermediate layer consisting of $Sn_{0.9}In_{0.1}P_2O_7$ and Pt/C catalyst powders at the interface between the electrolyte and cathode, which significantly reduced the cathode polarization. As a result, the peak power density reached 264 mW cm^{-2} at 250°C using the 0.35-mm-thick electrolyte. The present fuel cell also showed high stability at low relative humidities ($p_{H_2O} \approx 0.0075$ atm) and 10% CO concentration.
 [DOI: 10.1149/1.2183927]

Manuscript submitted December 9, 2005; revised manuscript received January 9, 2006. Available electronically March 27, 2006.

Proton exchange membrane fuel cells (PEMFCs) have received increasing interest in recent years because of their high efficiency and environmentally friendly characteristics. Proton-conducting fluoropolymers such as Nafion are commonly used as the electrolytes. However, these electrolytes need to be operated below 100°C, which causes serious CO poisoning of the anode electrocatalyst.[1,2] These electrolytes also require highly humidified conditions to achieve sufficient proton conductivity, and the use of the large water control unit required complicates fuel cell systems.[3,4] Such problems can obviously be avoided by using a proton conductor functioning as the electrolyte above 100°C under low humidity or dry atmosphere.

Anhydrous proton conductors for intermediate-temperature fuel cells (100–300°C) usually consist of oxyanions (SO_4^{2-} or PO_4^{3-}), in which an oxide ion joins with a proton by a hydrogen bond.[5-11] However, there is a temperature limitation on the use of sulfonate-based proton conductors due to thermal decomposition of the SO_4^{2-} ions above 200°C.[6] Thus, recent attention has increasingly focused on phosphate-based proton conductors, which are stable up to 200°C or higher.[7-11]

We have recently reported a promising anhydrous proton conductor, 10 mol % In^{3+}-doped SnP_2O_7 ($Sn_{0.9}In_{0.1}P_2O_7$), for electrochemical devices in the temperature range of interest.[12,13] In a previous paper,[13] SnP_2O_7 showed a cubic structure with SnO_6 octahedra and P_2O_7 units at the corners and the edges, respectively. Such closely packed P_2O_7 units could provide many proton bonding sites and associated transport pathways in the bulk, resulting in high proton conductivities above 0.1 S cm^{-1} between 150 and 350°C under unhumidified conditions. The electromotive force values of a hydrogen concentration cell with this material were very near the theoretical values calculated from Nernst's equation, indicating that the ionic transport number was 0.97. Thus, $Sn_{0.9}In_{0.1}P_2O_7$ was found to be an almost purely ionic conductor in hydrogen atmospheres.

In the present study, we used $Sn_{0.9}In_{0.1}P_2O_7$ as electrolyte material for intermediate-temperature fuel cells. Fuel cell tests were conducted in unhumidified hydrogen and air in the temperature range of 150–350°C. The internal resistances of the fuel cell were characterized in terms of the ohmic and polarization resistances. The dc conductivity values of the electrolyte were estimated from the IR drops during discharge and compared with the ac conductivity values reported in previous papers.[12,13] The cathode overpotential, occupying a large portion of the potential drop, was improved by placing an intermediate layer of $Sn_{0.9}In_{0.1}P_2O_7$ and Pt/C catalyst powders at the interface between the electrolyte and electrode. Finally, the tolerance of the fuel cell for CO was evaluated in the presence of 5 and 10% CO.

Experimental

Electrolyte preparation.— $Sn_{0.9}In_{0.1}P_2O_7$ was prepared as described in Ref. 13. Briefly, the corresponding oxides (SnO_2 and In_2O_3) were mixed with 85% H_3PO_4 and stirred at 300°C until a high-viscosity paste was formed. After calcinations of the paste in an alumina pot at 650°C for 2.5 h, the compound was ground with a mortar and pestle. The final P/(Sn + In) molar ratio of the compounds was confirmed to be 2.0 (±0.02) from X-ray fluorescence. The X-ray diffraction patterns of the compound were identical with those reported in the literature.[14] The compound powders were pressed into a pellet under a pressure of 2×10^3 kg cm^{-2}. The measured density of the obtained pellet was 3.065 g cm^{-3}, with a relative density of 79.3%.

Electrode and intermediate layer preparation.— Both the anode and cathode were made from a catalyst (10 wt % Pt/C, E-TEK) and carbon paper (Toray TGPH-090), in which the Pt loading was about 0.6 mg cm^{-2}. An intermediate layer was prepared by mixing $Sn_{0.9}In_{0.1}P_2O_7$ and Pt/C catalyst powders (the latter prepared in-house) with a 10% poly(vinylidene fluoride) binder in 1-methyl-2-pyrrolidinone solvent using a mortar and pestle. The preparation of the Pt/C catalysts (10–40 wt % Pt) was carried out as follows. Carbon powders (Ketjen BLACK EC600JD) were suspended in an ethanol/water solution. A chloroplatinic acid ($H_2PtCl_6 \cdot 6H_2O$) solution and sodium borohydride ($NaBH_4$) solution were simultaneously added into the suspension at 70°C with stirring. The mixture solution was stirred for 2 h and washed with distilled water repeatedly until the pH of the filtrate was roughly 7. After drying at 90°C overnight, the catalyst was heat-treated with a H_2/Ar (10 vol % H_2) atmosphere at 200°C for 1 h. The intermediate layer was applied homogeneously by doctor blading on the cathode. Microstructure of the intermediate layer was studied by scanning electron microscopy (SEM).

Fuel cell performance tests.— The anode and cathode (area: 0.5 cm^2) were set on both sides of the $Sn_{0.9}In_{0.1}P_2O_7$ electrolyte (1.0-mm thickness unless otherwise specified). Two gas chambers were set up by placing the cell between two alumina tubes. Each chamber was sealed with an inorganic adhesive. The fuel and air chambers were supplied with unhumidified hydrogen and air, respectively, at a flow rate of 30 mL min^{-1}. The current-voltage curves were measured by the four-probe method. The potential drop during discharge was analyzed by the current interruption method.

* Electrochemical Society Student Member.
** Electrochemical Society Active Member.
z E-mail: hibino@urban.env.nagoya-u.ac.jp

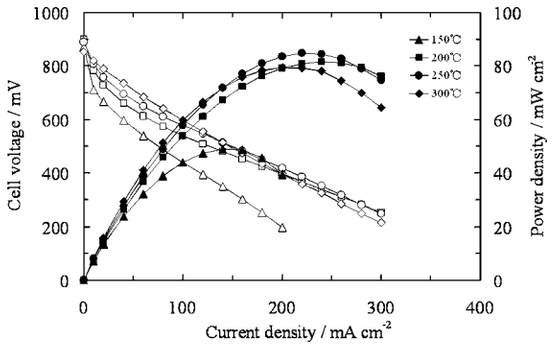

Figure 1. Cell voltage and power density vs current density of the fuel cells using $Sn_{0.9}In_{0.1}P_2O_7$ as the electrolyte between 150 and 300°C. Unhumidified hydrogen and air were supplied to the anode and cathode, respectively, at a flow rate of 30 mL min^{-1}.

In our case, a Pt reference electrode was attached on the surface of the side of the electrolyte. The electrode polarization was also investigated by measuring the impedance spectra between the cathode and reference electrodes. CO tolerance tests were performed by supplying hydrogen or a mixture of 5 or 10% CO and hydrogen to the fuel chamber.

Results and Discussion

Figure 1 plots the cell voltage and power density vs the current density at various temperatures using 10 wt % Pt/C (E-TEK) as the cathode under unhumidified conditions ($p_{H_2O} \approx 0.0075$ atm). The open-circuit voltages (OC) were about 920 mV, which was lower than the theoretical value of ~1.1 V. As reported earlier,[13] $Sn_{0.9}In_{0.1}P_2O_7$ was an almost purely ionic conductor in reducing atmospheres ($p_{O_2} = 10^{-22}$–10^{-3} atm), but showed mixed proton and electron-hole conduction in oxidizing atmospheres ($p_{O_2} = 10^{-3}$–1 atm). Thus, the low OC are attributable to the partial electron-hole conduction in the electrolyte, causing an internal short circuit in the cell. Another possible explanation is physical leakage of gas through the electrolyte since the OC increased with increasing electrolyte thickness. The fuel cell yielded the peak power density of 85 mW cm^{-2} at 250°C. However, this power density value was much lower when compared to that expected from the ac conductivity (1.95×10^{-1} S cm^{-1}) of the electrolyte reported earlier.[13]

To better understand the above low cell performance, the IR drops of fuel cells with $Sn_{0.9}In_{0.1}P_2O_7$ electrolytes of varying thickness were measured by the current interruption method. Figure 2a shows the IR drops of the electrolytes with thicknesses of 1.0, 1.5, and 2.0 mm measured between 150 and 300°C. The IR drops were primarily determined by the electrolyte thickness and were less dependent on the temperature. The dc conductivity values of the electrolyte were estimated from the IR drops and compared with the ac conductivity values. The results are shown in Fig. 2b. The dc conductivity values for the different electrolyte thicknesses were close to each other. At 250°C, for example, the dc conductivity values were 1.35, 1.43, and 1.41×10^{-1} S cm^{-1} for the electrolyte thicknesses of 1.0, 1.5, and 2.0 mm, respectively. Furthermore, the dc conductivity values were roughly in agreement with the ac conductivity values at all temperatures tested. The slight difference in conductivity between the dc and ac measurements is probably due to the contact resistance between the electrode and current collector. This agreement means that high proton conductivity values of $Sn_{0.9}In_{0.1}P_2O_7$ were demonstrated under fuel cell operation conditions. However, the contribution due to migration of oxide anions and/or alkaline cations to the measured conductivity values cannot

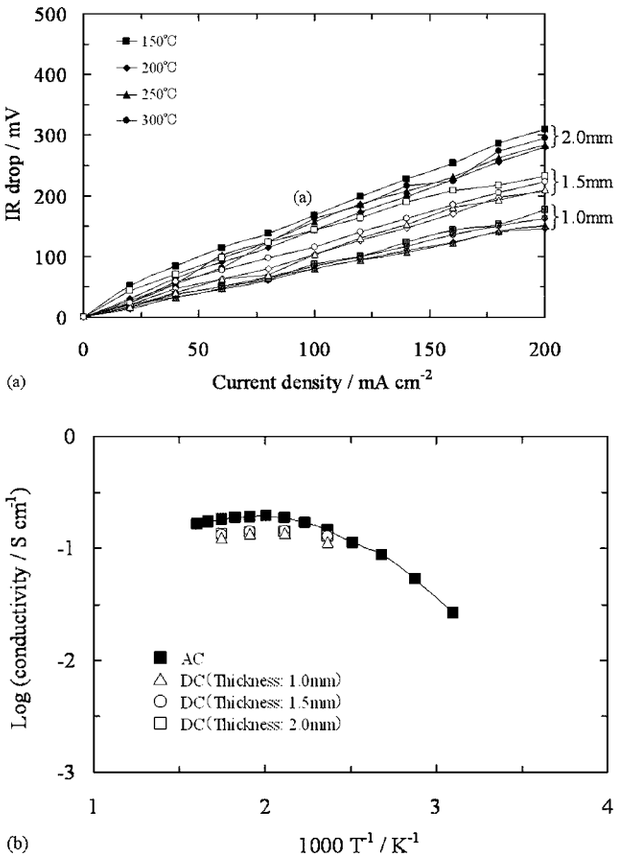

Figure 2. (a) IR drops of $Sn_{0.9}In_{0.1}P_2O_7$ electrolytes with thicknesses of 1.0, 1.5, and 2.0 mm between 150 and 300°C. (b) Comparison between dc and ac conductivity values of $Sn_{0.9}In_{0.1}P_2O_7$ electrolytes at various temperatures.

be excluded. The agreement between the dc and ac measurements also suggests that the low cell performance shown in Fig. 1 was caused by a large electrode polarization.

The electrode polarization was measured between 150 and 300°C. The anodic and cathodic overpotentials as a function of the current density are shown in Fig. 3. The cathodic overpotentials were much larger than the anodic overpotentials over the whole temperature range. Moreover, the cathodic overpotential showed a strong temperature dependence, suggesting that the cathode had a

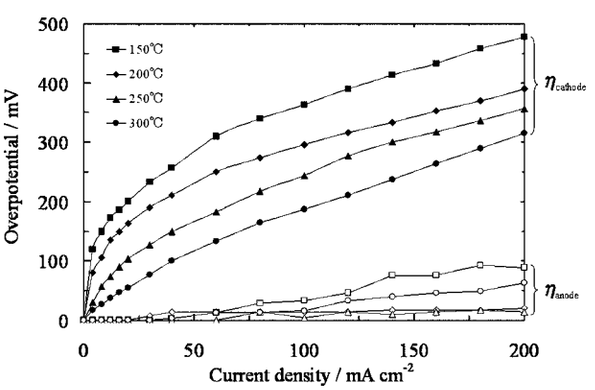

Figure 3. Anodic and cathodic overpotentials between 150 and 300°C.

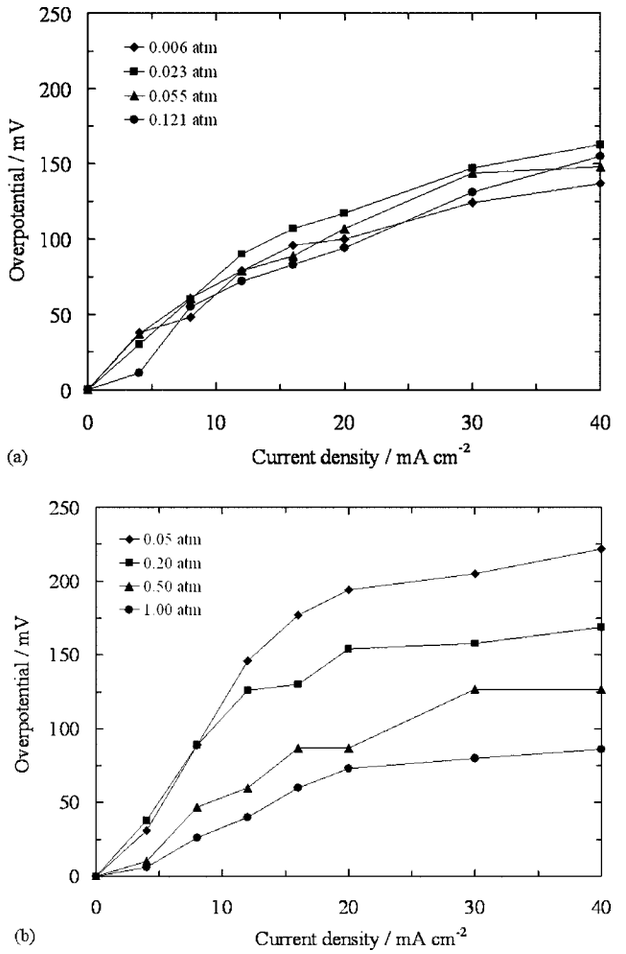

Figure 4. Cathodic overpotentials under various (a) p_{H_2O} and (b) p_{O_2} at 250°C.

high activation energy for the reduction of oxygen. Clearly, the development of a more active cathode is required to improve cell performance.

In order to determine the origin of the high overpotential at the cathode, the influence of p_{H_2O} and p_{O_2} on the cathodic overpotential was measured at 250°C. As shown in Fig. 4a, the cathodic overpotential was independent of p_{H_2O}, indicating that the water formed electrochemically does not affect the subsequent cathode reaction. This is presumably because the water formed is promptly desorbed from the electrode as water vapor under the present conditions. It can be seen from Fig. 4b that the cathodic overpotentials increased significantly with decreasing p_{O_2}. This result is mainly ascribed to the fact that the diffusion of oxygen through the electrode or its charge-transfer reaction at the electrolyte/electrode interface proceeds at a very slow rate. Another possible reason may be due to a decrease in p-type electronic conductivity of the electrolyte surface with decreasing p_{O_2}.

It is useful to increase the area of the three-phase boundary for promotion of the cathode reaction. Thus, intermediate layers of $Sn_{0.9}In_{0.1}P_2O_7$ and Pt/C catalyst powders were applied at the interface between the electrolyte and electrode. As a result of the optimization of both the Pt content in the Pt/C catalyst and the weight ratio of the $Sn_{0.9}In_{0.1}P_2O_7$ electrolyte to the Pt/C catalyst, the cathodic overpotential could be most improved when Pt content = 30 wt % and $Sn_{0.9}In_{0.1}P_2O_7$:Pt/C catalyst = 10:1 (Fig. 5). The microstructure of the intermediate layer is shown in Fig. 6. Agglomerates of the $Sn_{0.9}In_{0.1}P_2O_7$ electrolyte (agglomerate size: 400–500 nm) were homogeneously dispersed in the Pt/C catalyst powders. It is believed that the intermediate layer provides proton conduction to the cathode, enhancing the frequency of contact between proton and oxygen.

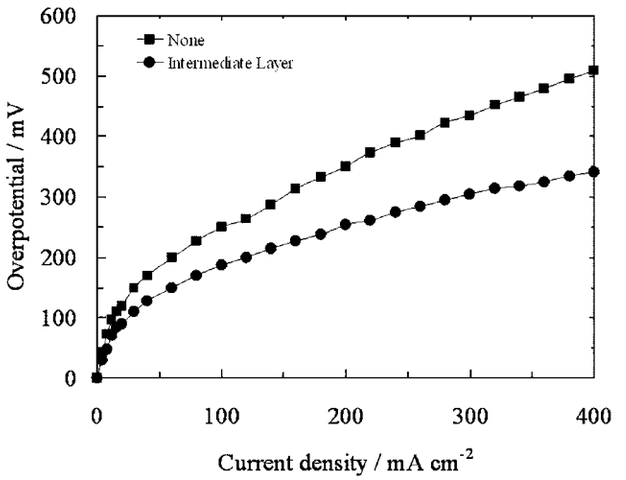

Figure 5. Cathodic overpotentials without and with an intermediate layer between the electrolyte and electrode. The intermediate layer is composed of $Sn_{0.9}In_{0.1}P_2O_7$ and 30 wt % Pt/C catalyst powders with a weight ratio of 10:1.

Performance of the fuel cell with the intermediate layer was evaluated under unhumidified conditions. The experimental conditions were the same as those shown in Fig. 1. The results are shown in Fig. 7a. The voltage drop during discharge was less dependent on the temperature between 200 and 300°C, which is responsible for the small difference in the proton conductivity of the electrolyte under such conditions. The peak power density ranged from 120 mW cm^{-2} at 150°C to 152 mW cm^{-2} at 250°C; these values are considerably higher than those obtained without using the intermediate layer shown in Fig. 1. This indicates that the intermediate layer effectively improved the cell performance. Another important contribution of this intermediate layer to cell performance was that the layer increased the proportion of the ohmic resistance in the whole internal resistance compared to the polarization resistance. As

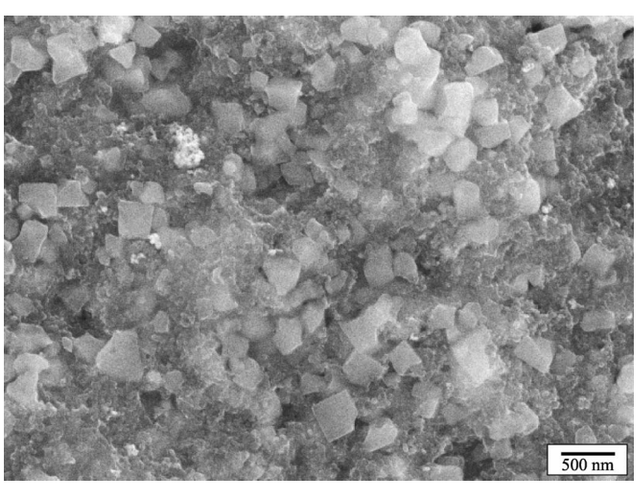

Figure 6. SEM micrograph of an intermediate layer of $Sn_{0.9}In_{0.1}P_2O_7$ and 30 wt % Pt/C catalyst powders.

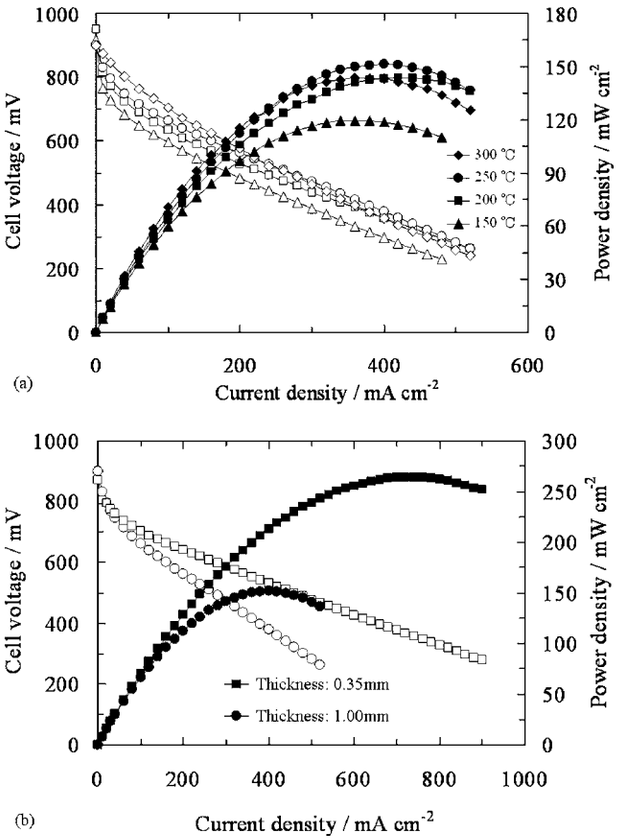

Figure 7. Performance of a fuel cell using $Sn_{0.9}In_{0.1}P_2O_7$ as the electrolyte with an intermediate layer of $Sn_{0.9}In_{0.1}P_2O_7$ and 30 wt % Pt/C catalyst. (a) Cell voltage and power density current density of the fuel cells between 150 and 300°C for an electrolyte thickness of 1.0 mm. (b) Cell voltage and power density current density of the fuel cells using electrolytes with different thicknesses at 250°C. The experimental conditions are the same as those shown in Fig. 1.

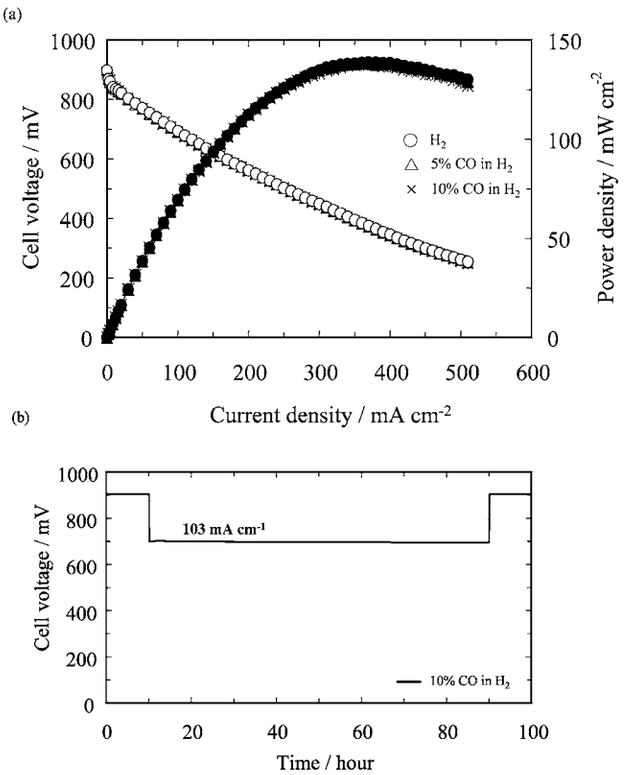

Figure 8. (a) Cell voltage and power density current density of the fuel cell using H_2 and a mixture of 5 or 10% CO + H_2 as the fuel gas at 250°C. (b) Stability of the fuel cell tested using a mixture of 10% CO + H_2 with the fuel gas at 250°C.

a result, the peak power density was enhanced to 264 mW cm^{-2} by reducing the electrolyte thickness to 0.35 mm at 250°C, as shown in Fig. 7b.

Finally, CO poisoning of the present fuel cell was investigated by supplying hydrogen or a mixture of 5 or 10% CO and hydrogen to the fuel chamber at 250°C. The cell performance was clearly not influenced by the presence of CO (Fig. 8a). Similar results were observed in ac impedance spectra, which maintained a constant polarization resistance regardless of the presence of CO. Such a negligibly small CO poisoning effect is roughly in agreement with theoretical studies on CO tolerance at high temperatures.[15] Short-term stability tests were also carried out in the presence of 10% CO at 250°C. The cell voltage was initially set to 700 mV by drawing current from the cell and then monitored with the current density maintained at a constant value. The cell voltage was almost stable for 60 h (Fig. 8b). These results indicate that the present fuel cell has excellent CO tolerance for actual applications, in which the CO concentration in the outlet gases from conventional reformers is usually 10%.[16]

The fuel cell with the $Sn_{0.9}In_{0.1}P_2O_7$ electrolyte exhibited a more stable performance at low relative humidities and high CO concentrations compared to PEMFCs, which makes fuel cell systems significantly simpler and more economic. Furthermore, the present fuel cell is expected have additional advantages over PEMFCs, such as higher reaction rates, faster heat rejection rates, and more efficient thermal utilization. These advantages would greatly enhance the position of intermediate-temperature fuel cells as the preferred power generation technology for practical applications.

Conclusions

Performance of a fuel cell that employs $Sn_{0.9}In_{0.1}P_2O_7$ as the electrolyte was evaluated at low relative humidities and in the temperature range of 150–300°C. The dc conductivity values estimated for the fuel cell were roughly in agreement with the ac conductivity values of the electrolyte over the whole temperature range, demonstrating the high proton conductivity of $Sn_{0.9}In_{0.1}P_2O_7$ under fuel cell operation conditions. The cathodic polarization was significantly improved by applying an intermediate layer of $Sn_{0.9}In_{0.1}P_2O_7$ and 30 wt % Pt/C catalyst powders at the interface between the electrolyte and cathode. The resulting power density reached 264 mW cm^{-2} at 250°C with the 0.35-mm-thick electrolyte. More importantly, the present fuel cell showed excellent tolerance for 10% CO and good thermal stability in unhumidified conditions.

Nogoya University assisted in meeting the publication costs of this article.

References

1. S. Malhotra and R. Datta, *J. Electrochem. Soc.*, **144**, L23 (1997).
2. Q. Li, R. He, J. A. Gao, J. O. Jensen, and N. J. Bjerrum, *J. Electrochem. Soc.*, **150**, A1599 (2003).
3. A. Karthikeyan, C. Martindale, and S. W. Martin, *J. Non-Cryst. Solids*, **349**, 215 (2004).
4. P. Berg, K. Promislow, J. S. Pierre, J. Stumper, and B. Wetton, *J. Electrochem. Soc.*, **151**, A341 (2004).
5. T. Uda, D. A. Boysen, and S. M. Haile, *Solid State Ionics*, **176**, 127 (2005).
6. S. M. Haile, D. A. Boysen, C. R. I. Chisholm, and R. B. Merle, *Nature (London)*,

410, 910 (2001).
7. T. Matsui, S. Takeshita, Y. Iriyama, T. Abe, M. Inaba, and Z. Ogumi, *Electrochem. Commun.*, **6**, 180 (2004).
8. D. A. Boysen, T. Uda, C. R. I. Chisholm, and S. M. Haile, *Science*, **303**, 68 (2004).
9. W. Wieczorek, G. Zukowska, R. Borkowska, S. H. Chung, and S. Greenbaum, *Electrochim. Acta*, **46**, 1427 (2001).
10. A. Matsuda, T. Kanzaki, K. Tadanaga, M. Tatsumisago, and T. Minami, *Solid State Ionics*, **154–155**, 687 (2002).
11. J. D. Kim and I. Honma, *Electrochim. Acta*, **49**, 3179 (2004).
12. M. Nagao, T. Yoshii, T. Hibino, M. Sano, and A. Tomita, *Electrochem. Solid-State Lett.*, **9**, J1 (2006).
13. M. Nagao, A. Takeuchi, P. Heo, T. Hibino, M. Sano, and A. Tomita, *Electrochem. Solid-State Lett.*, **9**, A105 (2006).
14. R. K. Gover, N. D. Withers, S. Allen, R. L. Withers, and J. S. O. Evans, *J. Solid State Chem.*, **166**, 42 (2002).
15. C. Yang, P. Costamagna, S. Srinivasan, J. Benziger, and A. B. Bocarsly, *J. Power Sources*, **103**, 1 (2001).
16. M. Levent, D. J. Gunn, and M. A. El-Bousiffi, *Int. J. Hydrogen Energy*, **28**, 945 (2003).